Italian Association of Aeronautics and Astronautics
XXVI International Congress
31st August – 3rd September 2021
On-line event hosted by the Tuscany AIDAA Section in Pisa

MACHINE LEARNING APPLICATIONS FOR AEROSPACE STRUCTURES ASSESSMENTS

F. Dipietrangelo[1*], F. Nicassio[1], G. Scarselli[1], G. Petrone[2], A. Casaburo[2], S. De Rosa[2]

[1]Department of Innovation Engineering, University of Salento, Lecce, Italy

[2]Department of Industrial Engineering, University of Naples "Federico II", Napoli, Italy

*flavio.dipietrangelo@unisalento.it

ABSTRACT

This work aims at determining the location of low speed impact events on thin aluminium panels, specifically designed to be used on typical aircraft fuselage and wing panels, by processing the acoustic emission signals. The detection principle is based on the propagation of the first antisymmetric Lamb wave (A_0 mode) in the panel by means of four piezoelectric (PZT) sensors are bonded to acquire the signals. The impact location is assessed with the use of a supervised machine learning algorithm that is based on linear regression, appropriately designated to post-process the acquired signals. Some experimental cases are reported in order to investigate the optimal kind and amount of training data to improve the performance of the algorithm and therefore the accuracy of the impact location estimation.

Keywords: Structural Health Monitoring, Machine Learning, Supervised learning, Impact localization

1 INTRODUCTION

During their operational life aircrafts, helicopters, launch vehicles and other aviation equipment can be subjected to impacts generated by external environmental sources. In some cases, high intensity impacts can be the cause for potential damage to the structure, representing a common risk in aviation security and have been the reason for many incidents and fatalities [1]. It is fundamental to periodically check the integrity of the structure and in this scenario Structural Health Monitoring (SHM) provides real time monitoring through an integrated sensors' network, that can detect acoustic emission caused by impacts or crack generation. Generally, the location of an impact requires the identification of an elastic wave feature, which varies depending on the impact at low speed. It is also necessary to find a correlation between this feature and the location where the impact occurred [2]. Impacts' location and the elastic wave features represent a dataset for the application of Machine Learning algorithms. These algorithms are designed to recognize patterns and regularities and to perform subsequent predictions automatically.

In this work, low speed impacts have been characterised in order to build a dataset of experimental measurements, on which supervised learning algorithms have been applied and, subsequently, compared to a typical triangulation method.

2 EXPERIMENTAL SETUP

2.1 Hardware equipment and software

The test setup of data acquisition for impact location has been performed with the tools reported in Figure 1. Impacts have been characterised by dropping a steel ball onto an aluminium plate, which was riveted on a metal support (the plate can be considered clamped at the edges). Four PZT sensors have been bonded on the surface of the plate to acquire the signal. Each of them has been connected to a separate channel of an oscilloscope, in order to observe the changes in the electrical signal over a period of time. Eventually, specific software (Picoscope, MATLAB) has been used to read and process the acquired data. Low speed impacts have been acquired using the drop tower shown in Figure 1 (b), which consists of a laser pointer and a guide duct, both mounted on a sliding channel. Impacts have been generated releasing a small steel ball (having a diameter of 2 mm) from a fixed height of 20 mm.

The monitored plate was made of aluminium alloy with density 2700 kg/m^3, elastic modulus E = 72 GPa and Poisson's ratio $\nu = 0.33$. The plate has been fixed on a metallic support by fasteners and its size was 250x250x1,2 mm. The location of the impact has been evaluated by using an array of four piezoelectric ceramic PZT $\mathrm{Pb}[Z_{r_x}\mathrm{Ti}_{1-x}]\mathrm{O}_3$ sensors.

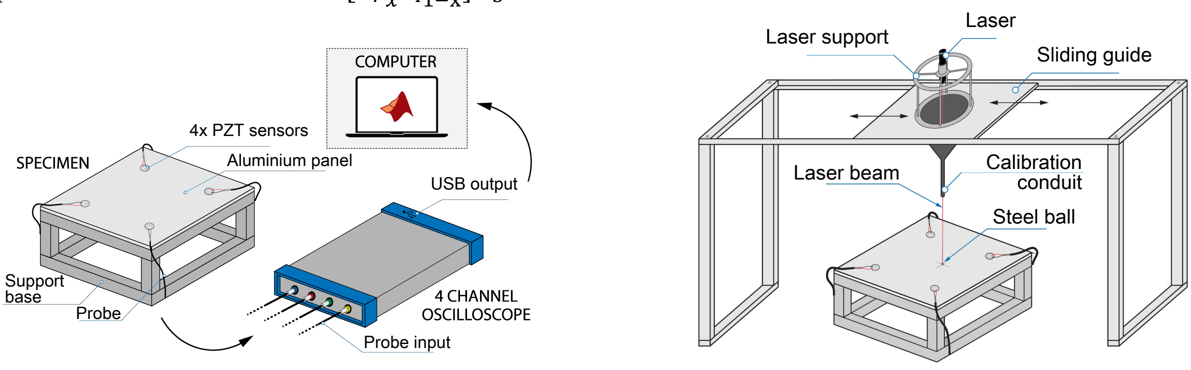

Figure 1: Experimental setup. (a): Acquisition system; (b) Drop tower for impact simulation.

2.2 Signals processing, data acquisition and time-of-flight estimation

An impact can be described as a Dirac delta function load acting on the structure, producing multiple Lamb modes at various frequencies (from zero to infinity) which propagate with different group velocities. The acoustic emission frequency-band in a thin plate occurs predominantly in the range of hundreds of kiloHertz, while at low frequencies, only the zero-modes (S_0 and A_0) can be [3]. When the structure is hit by foreign objects, it can be deformed most likely only when the impact direction is vertical to the plate's surface. Therefore, only this type of impact has been considered, while the acoustic emission has been related only to the A_0 mode because of its larger strain amplitude at low frequencies [4]. Figure 2 shows the tuning curves for the A_0 and S_0 modes, experimentally obtained by exciting an aluminium plate of similar thickness to that used in this work [5].

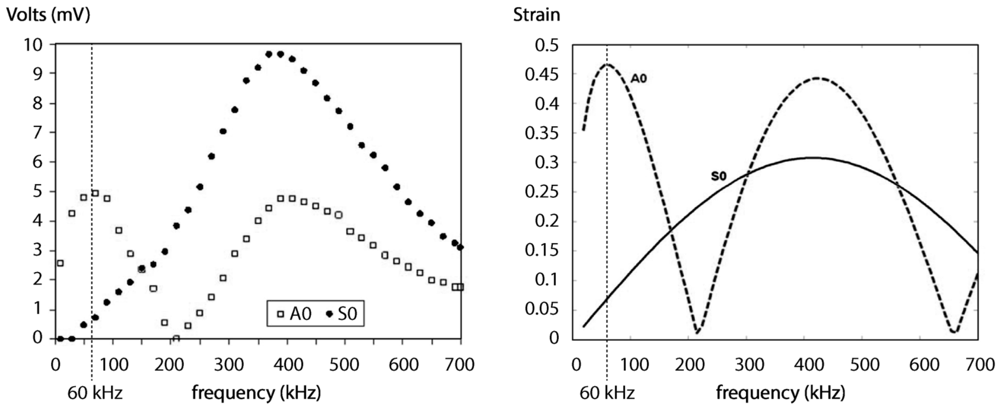

Figure 2: Lamb waves tuning curves for an aluminium plate of 1.1mm thickness and 7mm square PWAS [5].

It is possible to notice that the first maximum of the A_0 mode (of interest in this study) occurred at around 60 kHz: at this frequency the S0 mode is very small and the A_0 signal is dominant. For this reason, after the acquisition by an oscilloscope, the signals have been processed in MATLAB by a Short Time Fourier Transform (STFT) and filtered around 60 kHz. At this frequency the arrival time of the A_0 mode has been evaluated according to the procedure described in [6] for each sensor of the array. After the evaluation of the arrival time, also called Time of Flight (ToF), to each sensor, a dataset has been built, made of N samples (impacts points) and, for each sample, the actual coordinates (x,y) and the difference between the ToFs at three sensors and the ToF at one reference sensor.

3 PERFORMANCE ANALYSIS AND RESULTS

3.1 Linear and non-linear analysis

The machine learning algorithm considered for the analysis of the available dataset has been the linear regression, in which the output is represented by the vector of the two coordinates (*x,y*) as a linear function of the three ToF differences, weighted on the basis of a design matrix defined during the model training as defined in [7]. The first analysis has been carried out to test the influence of the number and configuration of training data on the algorithm's performance. The assumed key performance indicator has been the distance from the actual impact point to the estimated one. In accordance with the studies conducted by Jones in [8], this parametric study has proceeded as follows:

1. two training impact grids using different number of impacts, 45 and 117 impacts, spaced equally on the plate have been created;
2. the algorithm has been tested using both training grids separately on a set of 50 impacts, whose coordinates differed from those of the training sets;
3. the training grid giving the lowest mean radial distance error after the test phase has been chosen.

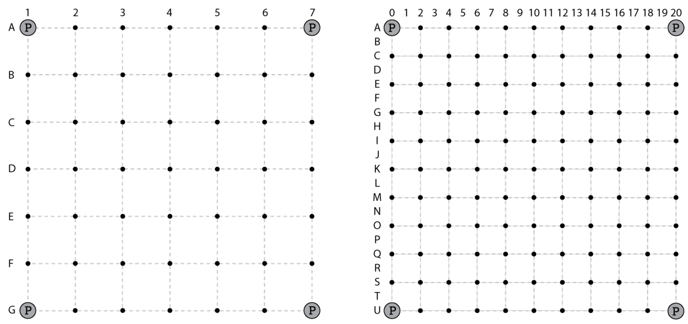

(a) (b)

Figure 3: Training impact grids. (a): 45-impacts grid; (b): 117-impacts grid.

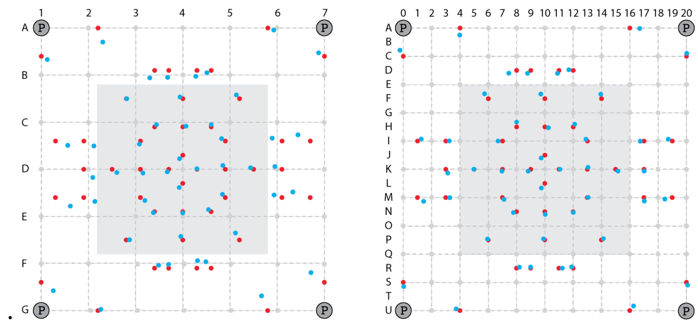

(a) (b)

Figure 4: Estimated impacts in relation to their exact location. (a): 45-impacts grid; (b): 117-impacts grid.

With reference to Figure 3 and Figure 4, black dots represent the impacted points for the training of the algorithm, red dots represent the impacted points for the test of the algorithm, blue dots: represent the test impact points estimated by the algorithm.

The results obtained in this first parametric study provide the following conclusions:

1. Higher training data improves the algorithm's performance: 37/50 impacts tested (74%) have been estimated with more accuracy (i.e. with the lowest radial error in millimeters) by using the rich-training grid. To provide a metric of the impact locations prediction accuracy, a Root-Mean-Square Error function E_{rms} has been defined, expressed for each data type as:

$$E_{rms} = \frac{1}{N}\sqrt{\sum_{i=1}^{N}(x - x_i)^2 + (y - y_i)^2} \qquad (1)$$

where N = 50 is the number of test impacts, (x,y) are the exact test impacts coordinates in millimeters and (x_i,y_i) the algorithm's solution for the impact coordinates in millimeters. The

following RMS errors have been obtained for the poor-training grid ($E_{rms,45}$) and the rich-training grid ($E_{rms,117}$): $E_{rms,45} = 3.07$ mm; $E_{rms,117} = 1.69$ mm.
The increase in training impacts from 45 to 117 has therefore led to an RMS error reduction equal to 45%. The maximum radial errors were equal to 7.62 mm for the test with the poor-training grid and 4.34 mm with the rich-training grid (-43%).

2. Non-uniform accuracy of the estimate on the plate surface: when separately analyzing the results obtained in the central zone (grey zone in Figure 4) and the border one, a discrepancy in the accuracy of the estimate is evident in both cases, as reported in Table 1.

The results show that the estimation is comparable in the central area of the plate, while in the border zone it is better training the model with the rich-training grid. A similar result has also been experienced by Liu et al. in [9], according to which the higher estimation errors in some areas of the plate depend on the location of the sensors and on the sensitivity of the wave ToFs differences used for the estimation during the validation phase. To overcome this limitation, the authors suggested the use of a multi-array sensor net. In order to improve the performances of the model in the border zone, a non-linear model has been considered, adding the squares and the double products of the ToF differences, obtaining a quadratic regression model, [3]. The impact test grid has been the same used for the previous cases, while the algorithm has been trained with the 117-impact grid. Table 2 reports the RMS errors obtained with the linear and non-linear models:

Impact zone	$E_{rms,45}$	$E_{rms,117}$
Overall	3.07 mm	1.69 mm
Center	1.62 mm	1.33 mm
Border	4.41 mm	2.03 mm

Table 1: RMS errors by zone.

Impact zone	$E_{rms,117}$ (NL)	$E_{rms,117}$ (L)
Overall	1.74 mm	1.69 mm
Center	1.79 mm	1.33 mm
Border	1.69 mm	2.03 mm

Table 2: RMS error comparison: Linear (L) vs Non-Linear (NL) model.

By comparing the results, it turns out that the overall RMS error obtained with the non-linear model is slightly greater. However, by separately analyzing the errors obtained for the central and border areas, it appears that:

1. the points located in the central area of the plate are better estimated with the linear model;
2. the points located in the border area of the plate are better estimated with the non-linear model, which allowed to obtain a reduction of the RMS error equal to 16,75%.

To this scope an approach to increase the algorithm's performance has been to use both models to estimate the location of the impact: the linear model for the impacts that occur in the central area, the non-linear model for the others, obtaining a mean error of 1.51 mm.

3.2 Triangulation method

In this last part of the study, a performance comparison with the triangulation-based algorithm adopted by Gunther et al. in [10] has been performed, in order to prove the existence of considerable advantages in using machine learning techniques for the localization of impacts compared to traditional methods. The triangulation algorithm used in this section has been provided by Carrino and is based in his studies [4]. A test with a set of 25 impacts has then been performed both for triangulation algorithm and for the machine learning one (based on the linear + non-linear model and trained with the 45-impact grid) and the RMS errors obtained for both methods are reported in Table 3:

Method	E_{rms}
Triangulation	4.32 mm
Machine Learning	2.96 mm

Table 3: RMS error comparison: Triangulation vs Machine Learning.

Below the complete results are summarised:

1. 12/25 impacts have been better estimated with the triangulation algorithm 13/25 with the machine learning algorithm;

2. as shown in Table 3, the RMS error obtained with the machine learning algorithm is 31,5% lower than the one obtained with the triangulation algorithm;
3. the maximum radial error reached with the triangulation method is 14.06 mm, while the maximum error reached with the machine learning algorithm is equal to 8.29 mm.

A further relevant issue with the triangulation method is its high error in the estimation of the impact location in proximity of the sensors. This issue did not occur with the machine learning algorithm, whose accuracy of the estimation remains approximately constant over the plate's surface.

4 CONCLUSIONS

This work focused on the development of a tool, capable of locating low speed impacts generated by foreign objects on aerospace structures (such as thin aluminium plates) with a sensors' array. Especially, the main studies have been focused on designing and optimizing machine learning-based algorithms to estimate the impact location. Linear and non-linear regression algorithms based on supervised learning have been considered for the purpose of this study. The training and test campaigns have been performed with more than 150 impacts: 1.51 mm is the best RMS error value (in terms of radial distances between the actual impact position and the estimated one), with non-linear algorithm for the border zone and linear algorithm for the centre one. A further comparison has been carried out between the combined non-linear/linear regression and the triangulation method. Although the latter is easier to be used (no training), the quality of the estimation is worse.

This work is a first step of a more complex study that is aimed to develop and test several machine learning-based algorithms with additional features like the structural damping (experimental campaign evaluation) and the sensors' location (modal approach and Chladni figures).

5 REFERENCES

[1] Roger Forsgren. The concorde accident: A case study. *Nasa aPPEL knowledge services* (2019).

[2] Yujie Ying, James Garrett, Irving Oppenheim, Lucio Soibelman, Joel Harley, Jun Shi, and Yuanwei Jin. Toward data-driven structural health monitoring: Application of machine learning and signal processing to damage detection. *J. Comput. Civil Eng.* (2013).

[3] Victor Giurgiutiu. *Structural health monitoring with piezoelectric wafer active sensors*. Elsevier, 1st edition (2007).

[4] Stefano Carrino, Francesco Nicassio, and Gennaro Scarselli. Development and application of an in-flight structural health monitoring system. *International congress on ultrasonics* (2019).

[5] Giola Santoni, Lucy Yu, Buli Xu, and Victor Giurgiutiu. Lamb wave mode tuning of piezoelectric wafer active sensors for structural health monitoring. *Journal of Vibration and Acoustics* (2007).

[6] Paul M. Schindler, Russell G. May, Richard O. Claus, and J. Kenneth Shaw. Location of impacts on composite panels by embedded fiber optic sensors and neural network processing. In William B. Spillman Jr., editor, *Smart Structures and Materials 1995: Smart Sensing, Processing, and Instrumentation*, volume 2444, pages 481 – 489. International Society for Optics and Photonics, SPIE (1995).

[7] C. M. Bishop. *Pattern recognition and Machine Learning*. Springer (2006)

[8] Richard T. Jones, James S. Sirkis, E. Joseph Friebele, and Alan D. Kersey. Location and magnitude of impact detection in composite plates using neural networks. In William B. Spillman Jr., editor, *Smart Structures and Materials 1995: Smart Sensing, Processing, and Instrumentation*, volume 2444, pages 469 – 480. International Society for Optics and Photonics, SPIE (1995).

[9] N. Liu. *Impact location on stiened composite structures using neural networks*. pages 395–408 (2001).

[10] Michael F. Gunther, Anbo Wang, Brian R. Fogg, Suzanne E. Starr, Kent A. Murphy, and Richard O. Claus. Fiber optic impact detection and location system embedded in a composite material. In Richard O. Claus and Robert S. Rogowski, editors, *Fiber Optic Smart Structures and Skins V*, volume 1798, pages 262 – 269. International Society for Optics and Photonics, SPIE, 1993.